Possible persistent ionization caused by giant blue jets

Nikolai G. Lehtinen[1] and Umran S. Inan[1]

Received 13 December 2006; revised 16 February 2007; accepted 26 February 2007; published 18 April 2007.

[1] We consider the possible production of persistent ionization at low altitudes ($h \leq 70$ km) by giant blue jets (GBJ), using a new five constituent model of stratospheric/lower-ionospheric chemistry. Results indicate substantial ionization at $h < 50$ km, which exhibits an initially rapid (few seconds) recovery due to electron attachment, followed by a long enduring recovery (>10 minutes) determined by the time scale of mutual neutralization of negative and positive ions. Such recovery signatures may be observable in subionospheric VLF data in the form of Early/fast events with long lasting recoveries. Analysis also indicates that electrons may sometimes be quickly ($\lesssim$1 ms) removed by the dissociative attachment mechanism in the presence of a high electric field, while the negative and positive ions remain and persist for extended periods of time. In such cases, the initial rapid recovery may not be observable in VLF data due to its typical time resolution of $\sim$10 to 20 ms. In stratosphere ($h \lesssim 50$ km) the ionization recovery is found to not be accurately described by a four-constituent model proposed by *Glukhov et al.*, (1992), hereinafter referred to as GPI, necessitating a fifth constituent, namely the heavy negative ions with high electron affinity (N_x^-).
Citation: Lehtinen, N. G., and U. S. Inan (2007), Possible persistent ionization caused by giant blue jets, *Geophys. Res. Lett.*, *34*, L08804, doi:10.1029/2006GL029051.

1. Introduction

[2] We consider the relaxation of ionization caused by GBJ, and the possibility of detection of such ionization as Early/fast perturbations on subionospherically propagating VLF signals. Blue jets are luminous discharges which start at cloud tops ($\sim$20 km), continue upward and stop around 40 km (see review by *Wescott et al.* [2001]), while the GBJ connect to the lower ionosphere, $h \sim 70$ km [*Pasko et al.*, 2002]. To describe the effect of GBJ on ionosphere and the perturbation of a VLF signal, we must model the time-dependent relaxation of ionization. There is a plethora of dynamic ionization models, which include, e.g., Glukhov-Pasko-Inan (GPI) model with 3 kinds of ions [*Glukhov et al.*, 1992], Zinn-Sutherland model with 9 species of negative and 23 species of positive ions, with 997 chemical reactions [*Zinn et al.*, 1990], Mitra-Rowe model with 6 kinds of ions [*Mitra*, 1975]. However, most of these models, even the most elaborate ones [*Zinn et al.*, 1990], have only been used above 50 km, and might not describe accurately the relaxation of ionization in the stratosphere ($h < 50$ km). In this paper we extend the GPI model to be applicable at lower altitudes by considering two different species of negative ions.

2. Upper Atmospheric Chemistry Model

2.1. GPI Model Overview

[3] The GPI model of lower ionosphere relaxation [*Glukhov et al.*, 1992; *Pasko and Inan*, 1994; *Rodriguez and Inan*, 1994] groups all charged particles into four constituents: electrons (density denoted by N_e), negative ions (N^-), light positive ions, such as O_2^+, NO^+ and N_2^+ (N^+), and heavy positive ions (clusters), such as $H^+(H_2O)_n$ (N_x^+). The evolution of these species is described by equations (1)–(5) below, with exclusion of equation (3) and $A \equiv 0$, $N_x^- \equiv 0$ in all others. This model grossly overestimates background electron densities below stratopause ($h \lesssim 50$ km). For example, *Glukhov et al.* [1992, Figure 3] suggest that at $h = 30$ km, the background electron density is $N_e \simeq 10^{-4} N^-$. Using $N_{\rm ion} \simeq 10^3$ cm^{-3} [*Mitchell and Hale*, 1973], we find a grossly overestimated value of $N_e \simeq 0.1$ cm^{-3}. At this electron density, most of the atmospheric conductivity would be due to electrons, but it is well known that the conductivity in the stratosphere is largely due to ions [*MacGorman and Rust*, 1998, p. 34].

2.2. Extension of the GPI Model

[4] At $h \lesssim 50$ km it is necessary to extend the GPI model by separating all negative ions into two groups. The first group are the light negative ions (density denoted N^-) formed by the attachment of electrons, including such ions as O_2^- and O^-, which have relatively low electron affinity. The second group (N_x^-) encompasses heavy negative ions into which N^- are converted by interacting with neutral species, such as NO_3^- and its hydrates $NO_3^-(H_2O)_n$. This conversion is important in the D region and even more important in the stratosphere ($\lesssim$50 km) [*Ferguson*, 1979]. Heavy negative ions have a very high electron affinity (3.91 eV for NO_3^- and even higher for the hydrates) [*Reid*, 1979], making electron detachment virtually impossible. The equations of ionization evolution are:

$$\frac{dN_e}{dt} = Q - \beta N_e + \gamma N^- + \gamma_x N_x^- - \left(\alpha_d N^+ + \alpha_d^c N_x^+\right) N_e \quad (1)$$

$$\frac{dN^-}{dt} = \beta N_e - \gamma N^- - \alpha_i \left(N^+ + N_x^+\right) N^- - A N^- \quad (2)$$

$$\frac{dN_x^-}{dt} = -\gamma_x N_x^- - \alpha_i \left(N^+ + N_x^+\right) N_x^- + A N^- \quad (3)$$

$$\frac{dN^+}{dt} = Q - \alpha_d N_e N^+ - \alpha_i \left(N^- + N_x^-\right) N^+ - B N^+ \quad (4)$$

$$\frac{dN_x^+}{dt} = -\alpha_d^c N_e N_x^+ - \alpha_i \left(N^- + N_x^-\right) N_x^+ + B N^+ \quad (5)$$

[1]Department of Electrical Engineering, Stanford University, Stanford, California, USA.

0094-8276/07/2006GL029051$05.00

One of the equations is dependent on others because of the neutrality condition $N^+ + N_x^+ = N_e + N^- + N_x^-$. The source of ionization Q (producing N_e and N^+) is due to a variety of processes [*Reid*, 1979]. For simplicity, we take the steady-state electron density N_e in D region from the IRI model [*Bilitza*, 2001] (available at http://modelweb.gsfc.nasa.gov/models/iri.html), and calculate the source that would produce it. In the stratosphere N_e is negligible and is not available from the IRI model. At these altitudes, we assume a cosmic ray source of radiation given by a simple formula (roughly accounting for cosmic ray flux attenuation through atmosphere and the fact that $Q_{\rm cr} \propto N \times$ cosmic ray flux):

$$Q_{\rm cr} = Q_p (N/N_p) e^{1-N/N_p}$$

where N is the total density of neutrals, N_p is the neutral density at the ionization production peak altitude h_p, Q_p is the maximum value of $Q_{\rm cr}$. We take values appropriate for mid-latitudes: $h_p \simeq 15$ km and $Q_p \simeq 10$ cm^{-3} s^{-1} [*Reid*, 1979].

[5] Most of the coefficients in equations (1)–(5) are the same as in the GPI model [*Glukhov et al.*, 1992] (all densities are in cm^{-3}):

[6] 1. Mutual neutralization coefficient $\alpha_i \simeq (10^{-7} + 10^{-24}N)$ cm^3 s^{-1}, with a term added to the constant value of *Glukhov et al.* [1992], based on the suggestion by *Mitchell and Hale* [1973] that three-body mutual neutralization process is dominant at $h \lesssim 40$ km.

[7] 2. Dissociative recombination coefficients $\alpha_d \simeq 10^{-7}$–3×10^{-7} cm^3 s^{-1} and $\alpha_d^c \simeq 10^{-6}$–$10^{-5}$ cm^3 s^{-1} [*Glukhov et al.*, 1992; *Florescu-Mitchell and Mitchell*, 2006].

[8] 3. Attachment rate $\beta = \beta_2 + \beta_3$, where β_2 and β_3 are rates of 2- and 3-body processes, respectively. The rate of 3-body process $\beta_3 \simeq 6 \times 10^{-32} N^2$ is obtained from a temperature-dependent formula of *Glukhov et al.* [1992] with $T = 200$ K and atmosphere constituent concentrations $N[{\rm O_2}]/N \simeq 0.2$, $N[{\rm N_2}]/N \simeq 0.8$. The temperature dependence of β_3 is $\sim e^{-600/T}/T$ and is weaker than that of γ (see below). In the presence of a high electric field, attachment is mostly due to a two-body dissociative process, the effective coefficient for which is [*Pasko et al.*, 1997]:

$$\beta_2 = \max\{0, \quad -9.3\times10^{-12} + 2.1\times10^{-13}(E/N) - 9.2\times10^{-16}(E/N)^2\} N \text{ s}^{-1} \quad (6)$$

where E/N is given in townsends (1 Td = 10^{-17} V cm^2). The value of β_2 peaks around the breakdown field of ~100–130 Td.

[9] 4. Detachment rate

$$\gamma \simeq \left(8.6\times10^{-10} e^{-6000/T} N + 2.5\times10^{-10} N_{\rm ac}\right) \text{s}^{-1} \quad (7)$$

The first term describes detachment by O_2 [*Kozlov et al.*, 1988; *Aleksandrov et al.*, 1997], while the second represents detachment by active species $N_{\rm ac} = N[{\rm O}] + N[{\rm N}] + N[{\rm O_2}(a^1\Delta_g)]$ [*Aleksandrov et al.*, 1997; *Gurevich*, 1978, p. 115]. The very sensitive temperature dependence of the first term is determined by the electron affinity of O_2^-, which is ~0.43 eV [*Herzenberg*, 1969]. This dependence makes the value of γ very uncertain within a few orders of magnitude [*Pasko and Inan*, 1994]. At nighttime, the second term is only important at >70 km [*Jursa*, 1985, pp. 21–43], not very relevant for the present paper. For daytime ionosphere, one should also consider photodetachment, the coefficient of which has a constant value of 0.33 s^{-1} [*Kozlov et al.*, 1988] to 0.44 s^{-1} [*Gurevich*, 1978, p. 114].

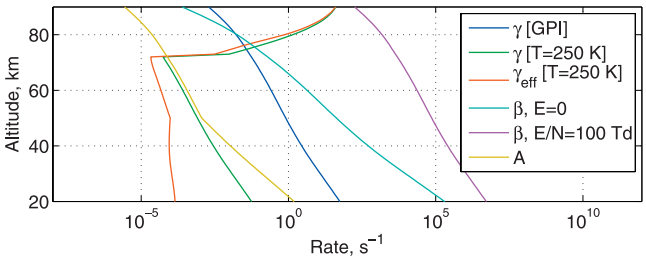

Figure 1. Detachment and attachment coefficients. The [GPI] value refers to $\gamma = 3 \times 10^{-17} N$ s^{-1} from [*Glukhov et al.*, 1992]; other values are calculated from equations (7) and (11). Increase of γ at $h > 70$ km is due to the active species, i.e., the second term of equation (7). Attachment rate β and $N^- \rightarrow N_x^-$ conversion rate A are also shown.

[10] 5. Rate of conversion of N^+ into N_x^+, $B = 10^{-31} N^2$ s^{-1} [*Glukhov et al.*, 1992].

[11] The new coefficients are:

[12] 1. Detachment rate from heavy negative ions $\gamma_x = 0$ at nighttime and $\gamma_x = 0.002$ s^{-1} due to photodetachment at daytime [*Reid*, 1979]. In the Mitra-Rowe model [*Mitra*, 1975], the analogous coefficient was assumed to have a nonzero value at nighttime.

[13] 2. Rate of conversion of N^- into N_x^-, denoted by A. We consider reaction

$$CO_3^- + NO \rightarrow NO_2^- + CO_2$$

proceeding with the rate of $\sim 10^{-11}$ cm^3 s^{-1} [*Fehsenfeld and Ferguson*, 1974]. We estimate $N[{\rm NO}]$ from *Zinn et al.* [1990, Figure B1] and obtain $A \simeq 3 \times 10^{-20} N$ s^{-1}–$10^{-18} N$ s^{-1} (see Figure 1). In the work of *Mitra* [1975], an analogous rate was denoted as $\bar{X}$ but the products of the relevant reaction were intermediate ions (denoted X^- in the same paper), such as CO_3^-.

2.3. Background Densities

[14] Some insight into equations (1)–(5) for background conditions can be gained by considering a simpler 3-constituent model [*Rishbeth and Garriott*, 1969, p. 110] with $N_t^+ = N^+ + N_x^+$ and $N_t^- = N^- + N_x^-$:

$$\frac{dN_e}{dt} = Q - \beta N_e + \gamma_{\rm eff} N_t^- - \alpha_{d,\rm eff} N_t^+ N_e \quad (8)$$

$$\frac{dN^-tot}{dt} = \beta N_e - \gamma_{\rm eff} N_t^- - \alpha_i N_t^+ N^-tot \quad (9)$$

$$\frac{dN_t^+}{dt} = Q - \alpha_{d,\rm eff} N_e N_t^+ - \alpha_i N^-tot N_t^+ \quad (10)$$

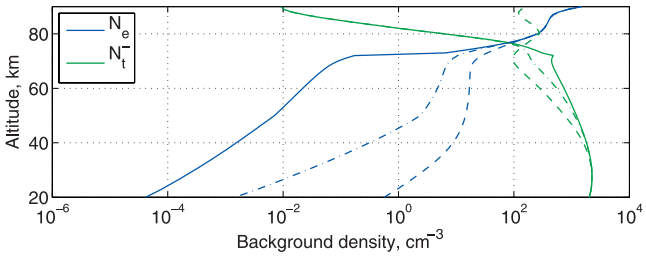

Figure 2. Background densities N_e, N_t^- calculated using the proposed 5-species model (solid) for with γ given by equation (7) for T = 250 K and GPI 4-species model (dashed) with $\gamma = 3 \times 10^{-17} N$ s^{-1} [*Glukhov et al.*, 1992]. The proposed five-species model still gives a much lower result for T = 350 K (dash-dotted curve for N_e), when the first term in equation (7) is equal to the GPI value of γ.

where the effective detachment coefficient γ_{eff} and effective dissociative recombination coefficient $\alpha_{d,\text{eff}}$ are weighted by relative concentrations of different kinds of ions:

$$\gamma_{\text{eff}} = \frac{\gamma N^- + \gamma_x N_x^-}{N^- + N_X^-} \tag{11}$$

$$\alpha_{d,\text{eff}} = \frac{\alpha_d N^+ + \alpha_d^c N_x^+}{N^+ + N_x^+} \tag{12}$$

The fact that $\gamma_x \simeq 0$ at nighttime and $N_x^- \gg N^-$ in stratosphere ($h \lesssim 50$ km) makes γ_{eff} negligible (see Figure 1), consistent with the conclusion by *Mitchell and Hale* [1973]. The coefficients α_d and α_d^c are constants independent of h, making the variations of $\alpha_{d,\text{eff}}$ not as dramatic as that of γ_{eff}. Various values of γ, γ_{eff} are shown in Figure 1. The GPI value of $\gamma = 3 \times 10^{-17} N$ s^{-1} corresponds to the first term of equation (7) for a relatively high background temperature $T \simeq 350$ K, a typical temperature for the lower thermosphere, much higher than the temperature range at the altitudes considered herein. In this paper, we use T = 250 K, an upper boundary for a wide range of altitudes including the stratosphere and mesosphere, with the possible exception of the stratopause (~50 km). The first term of equation (7) is then $3 \times 10^{-20} N$ s^{-1}.

[15] The steady-state negative ion ratio λ [*Rishbeth and Garriott*, 1969, p. 110] can be calculated from equations (8)–(10):

$$\lambda \equiv \frac{N_t^-}{N_e} = \frac{\beta}{\gamma_{\text{eff}} + \alpha_i N_t^+}$$

When $\gamma_{\text{eff}} \simeq 0$, this expression gives the electron density in the stratosphere at nighttime $N_e = \alpha_i N_{\text{ion}}^2/\beta \simeq 1.7 \times 10^{13} N^{-1}$ cm^{-3}, where we used $N_{\text{ion}} \simeq 10^3$ cm^{-3} [*Mitchell and Hale*, 1973; *MacGorman and Rust*, 1998, p. 34]. Comparison of the new five constituent model and the GPI model is demonstrated in Figure 2, where we once again use *Glukhov et al.*'s [1992] value of $\gamma = 3 \times 10^{-17} N$ s^{-1}. A large difference in the calculated electron densities at stratospheric altitudes is evident.

3. Conductivity and VLF Absorption

[16] We assume that GBJ produces initial ionization of $\Delta N_{e0} = 10^4$ cm^{-3} (with an equal value of ΔN_0^+), throughout a wide altitude range of 20 to 70 km. This assumption is rather arbitrary but is sufficient for our purposes, since we are interested in the persistence of the ionization in time rather than the absolute amount of ionization produced. The value of ΔN_{e0} is chosen to be only ~1–10 times higher than the stratospheric ion density, so that this perturbation does not have nonlinear effects which are large enough to change the qualitative chemistry of relaxation. Also, since the processes we are interested are relatively quick, there is no interaction between different altitudes.

[17] The relaxation of the ionization consists of two stages. In the first stage, free electrons are attached to create a population of N_t^-. This process works fastest if there is no detachment, as is the case when $\gamma \simeq 0$ or N^- are quickly converted to N_x^- (with time scale determined by A^{-1}), so that $\gamma_{\text{eff}} \simeq 0$. The time scale of the first stage is then $\tau_1 \simeq \beta^{-1}$ (see Figure 1 for the altitude dependence of these scales, with and without an electric field). In the second stage, the positive and negative ions recombine, with a time scale of $\tau_2 \sim (\alpha_i N_{\text{ion}})^{-1} \simeq 10^4$ s (we used $N_{\text{ion}} \simeq 10^3$ cm^{-3} and $\alpha_i \simeq 10^{-7}$ cm^3 s^{-1}). This long recovery time scale would be observable in subionospheric VLF data as a recovery lasting many minutes to tens of minutes. The initial stage, on the other hand, would be observable as a rapid initial partial recovery lasting only a few seconds. However, the first stage of rapid recovery may sometimes not be observable, when the value of the attachment coefficient β is high, so that τ_1 is too small to be detected within the time resolution of subionospheric narrowband VLF measurements (typically ~10 to 20 ms). Such high values of β might result from the high electric field (see equation (6)) which is undoubtedly present during the GBJ event.

3.1. Electrical Conductivity

[18] We calculate the conductivity from the electron and ion concentrations as

$$\sigma = \sum_{\text{species}} N_s e \mu_s$$

where N_s is one of the species (N_e, N^+, N^-, N_x^+ or N_x^-), and μ_s is the mobility of the species. We take the electron and ion mobilities as $\mu_e \simeq 1.36 \times 10^4 (N_0/N)$ cm^2 V^{-1} s^{-1} [*Pasko et al.*, 1997] and $\mu_{\text{ion}} \simeq 2.3 (N_0/N)$ cm^2 V^{-1} s^{-1} [*Hõrrak et al.*, 2000], with $N_0 \simeq 2.5 \times 10^{19}$ cm^{-3} being the

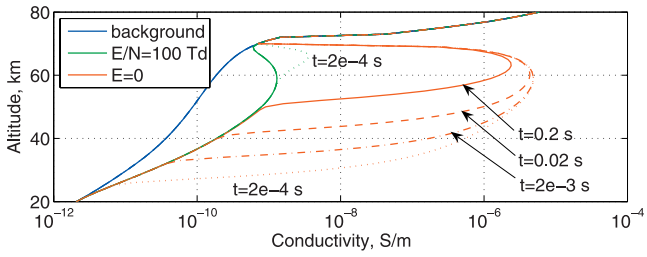

Figure 3. Average conductivity evolution during the first stage of ionization relaxation, with and without electric field. The line style denotes time: $t = 2 \times 10^{-4}$ s (dotted); $t = 2 \times 10^{-3}$ s (dash-dotted); $t = 2 \times 10^{-2}$ s (dashed); $t = 0.2$ s (solid).

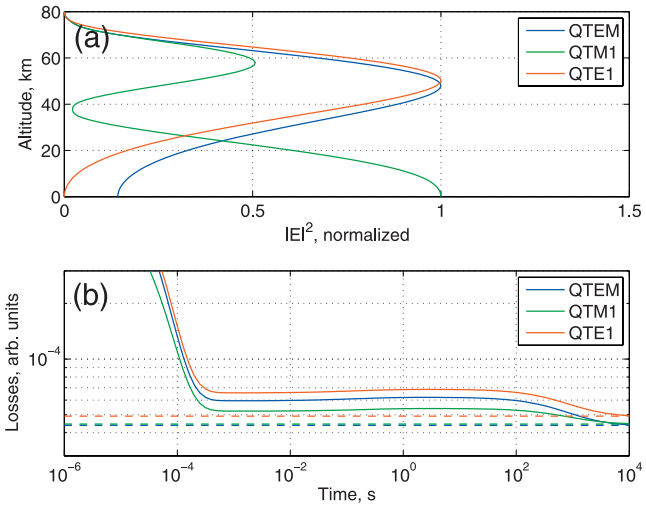

Figure 4. (a) Three lowest modes for the used background conductivity profile; (b) losses as a function of time.

atmospheric density at the sea level. In the presence of a high electric field, the electron conductivity is reduced (by a factor ~50 for E/N = 100 Td). Figure 3 shows the conductivity profiles for different moments of time. The plotted value is actually $\langle\sigma\rangle$, the conductivity averaged over the lateral horizontal area of the GBJ; we assume that the lateral area occupied by the GBJ grows from zero at h = 20 km to a maximum at h = 50 km and gradually decreases to zero again at h = 70 km. The absolute value of the lateral area is not important for our purpose of calculating the temporal dynamics; Figure 3 shows normalized $\langle\sigma\rangle$ so that $\langle\sigma\rangle = \sigma$ at the maximum lateral area of the GBJ. The assumption of the area decreasing from 50 km to 70 km is made to avoid discontinuity in $\langle\sigma\rangle$ and is not otherwise important. Figure 3 shows that in the presence of a high electric field, the conductivity relaxes to an intermediate state much faster due to higher values of the attachment coefficient β_2, so that all curves for $t \geq 2 \times 10^{-3}$ s look the same. Under these circumstances, subionospheric VLF data would not exhibit a rapid initial recovery but would only show the extended long enduring recovery.

3.2. Estimation of VLF Absorption Losses

[19] We proceed to provide a crude estimate of the VLF absorption losses as a function of time as $\int\langle\sigma\rangle\, w(h)\, dh$, the conductivity averaged over the horizontal area of the GBJ and then over altitudes with a weight function $w(h)$. As an estimate of $w(h)$, we take $|E|^2$, where $E(h)$ is the electric field structure in asubionospheric VLF mode (normalized, in arbitrary units). We calculate the electric field distribution in the first 3 Earth-ionosphere waveguide modes (QTEM, QTM1 and QTE1) by using an algorithm from *Wait* [1970, pp. 10–17] for isotropic media, taking also into account the curvature of the Earth. For nighttime ionosphere this algorithm can result in large errors due to anisotropicity of the conductivity tensor, but should be sufficient here for our purposes of providing a weighting function. The estimated mode structure is shown in Figure 4 a in terms of the altitude distribution of the total electric field.

[20] The time evolution of losses is shown in Figure 4b, in which we assume that the high electric field is shut off after t = 2 ms, i.e., upon the termination of the electron attachment process (see Figure 3). Once again, we see the long enduring recovery is well exhibited, but that the initial rapid recovery only lasts for the first few ms, which would not be detectable in typical subionospheric VLF data (having resolution of ~10 to 20 ms).

4. Discussion and Conclusions

[21] Results of a simple five constituent model of stratospheric/lower ionospheric chemistry indicates that ionization produced in GBJ may persist for tens of minutes, especially at stratospheric altitudes. The primary reason for it is the slow process of the mutual neutralization of stratospheric ions. The time scale of the subionospheric VLF amplitude relaxation in Early/fast VLF events associated with GBJs would thus be $\sim 10^3$–10^4 s, same as that of mutual neutralization of ions in stratosphere. Under normal circumstances, the long enduring recovery would be preceded by a rapid initial partial recovery (few seconds) due to the attachment of free electrons in the same altitude range. However, the attachment rate β may sometimes be exceptionally rapid due to the removal of these electrons by the two-body attachment mechanism induced by the high electric field during the GBJ event. This process could be simultaneous with the discharge that is represented by the luminous structure of the GBJ, and full modeling of the streamers, such as that of *Aleksandrov et al.* [1997], is necessary to validate this hypothesis.

[22] A similar initial ionization can be due to large red sprites which occur at the same range of altitudes (20–70 km). Modelling of streamers [*Babaeva and Naidis*, 1997; *Pasko et al.*, 1998] suggests ionization levels of $\sim 10^{14}(N/N_0)^2$ cm^{-3} in the streamer channels. Taking this as ΔN_{e0} produces similar temporal behavior of ionization relaxation. Exact value of ΔN_{e0} due to blue jets and sprites has to be described by full modelling of streamers and is beyond the scope of this article.

[23] The density of active species (atomic species O, N, and the metastable $O_2(a^1\Delta_g)$ molecule) was assumed constant in our model. However, we recognize herein that the number of active species might also be increased during the GBJ, simultaneously with ionization [*Kozlov et al.*, 1988; *Aleksandrov et al.*, 1997]. such an increase would lead to a higher detachment rate (7), and therefore to different ionization dynamics.

[24] **Acknowledgments.** This work was supported by the Office of Naval Research (ONR) under grant N00014-03-1-0333-PO0005 and the National Science Foundation under grant ATM-0535461.

References

Aleksandrov, N. L., E. M. Bazelyan, I. V. Kochetov, and N. A. Dyatko (1997), The ionization kinetics and electric field in the leader channel in long air gaps, *J. Phys. D Appl. Phys.*, *30*, 1616–1624, doi:10.1088/00223727/30/11/011.

Babaeva, N. Y., and G. V. Naidis (1997), Dynamics of positive and negative streamers in air in weak uniform electric fields, *IEEE Trans. Plasma Sci.*, *25*(2), 375–379, doi:10.1109/27.602514.

Bilitza, D. (2001), International reference ionosphere 2000, *Radio Sci.*, *36*, 261–271.

Fehsenfeld, F. C., and E. E. Ferguson (1974), Laboratory studies of negative ion reactions with atmospheric trace constituents, *J. Chem. Phys.*, *61*(8), 3181–3193.

Ferguson, E. E. (1979), Ion chemistry of the middle atmosphere, *NASA Conf. Publ., CP-2090*, 71–88.

Florescu-Mitchell, A. I., and J. B. A. Mitchell (2006), Dissociative recombination, *Phys. Rep.*, *430*(5–6), 277–374.

Glukhov, V. S., V. P. Pasko, and U. S. Inan (1992), Relaxation of transient lower ionospheric disturbances caused by lightning-whistler-induced electron precipitation bursts, *J. Geophys. Res.*, *97*, 16,971–16,979.

Gurevich, A. V. (1978), *Nonlinear Phenomena in the Ionosphere*, Springer, New York.

Herzenberg, A. (1969), Attachment of slow electron to oxygen molecules, *J. Chem. Phys.*, *51*(11), 4942–4950.

Hõrrak, U., J. Salm, and H. Tammet (2000), Statistical characterization of air ion mobility spectra at Tahkuse Observatory: Classification of air ions, *J. Geophys. Res.*, *105*, 9291–9302.

Jursa, A. S. (Ed.) (1985), *Handbook of Geophysics and the Space Environment*, Air Force Geophys. Lab., Springfield, Va.

Kozlov, S. I., V. A. Vlaskov, and N. V. Smirnova (1988), Specialized aeronomic model for investigating artificial midification of the middle atmosphere and lower ionosphere. 1. Requirements of the model and basic concepts of its formation, *Cosmic Res., Engl. Transl.*, *26*, 635–642.

MacGorman, D. R., and W. D. Rust (1998), *The Electrical Nature of Storms*, Oxford Univ. Press, New York.

Mitchell, J. D., and L. C. Hale (1973), Observations of the lowest ionosphere, *Space Res.*, *13*, 471–476.

Mitra, A. P. (1975), *D*-region in disturbed conditions, including flares and energetic particles, *J. Atmos. Terr. Phys.*, *37*, 895–913.

Pasko, V. P., and U. S. Inan (1994), Recovery signatures of lightning-associated VLF perturbations as a measure of the lower ionosphere, *J. Geophys. Res.*, *99*, 17,523–17,538.

Pasko, V. P., U. S. Inan, T. F. Bell, and Y. N. Taranenko (1997), Sprites produced by quasi-electrostatic heating and ionization in the lower ionosphere, *J. Geophys. Res.*, *102*, 4529–4562.

Pasko, V. P., U. S. Inan, and T. F. Bell (1998), Spatial structure of sprites, *Geophys. Res. Lett.*, *25*, 2123–2126.

Pasko, V. P., M. A. Stanley, J. D. Mathews, U. S. Inan, and T. G. Wood (2002), Electrical discharge from a thundercloud top to the lower ionosphere, *Nature*, *416*(6877), 152–154, doi:10.1038/416152a.

Reid, G. C. (1979), The middle atmosphere, *NASA Conf. Publ.*, *CP-2090*, 27–42.

Rishbeth, H., and O. W. Garriott (1969), *Introduction to Ionospheric Physics*, Elsevier, New York.

Rodriguez, J. V., and U. S. Inan (1994), Electron density changes in the nighttime D region due to heating by very-low-frequency transmitters, *Geophys. Res. Lett.*, *21*, 93–96.

Wait, J. R. (1970), *Electromagnetic Waves in Stratified Media*, 2nd ed., Elsevier, New York.

Wescott, E. M., D. D. Sentman, H. C. Stenbaek-Nielsen, P. Huet, M. J. Heavner, and D. R. Moudry (2001), New evidence for the brightness and ionization of blue starters and blue jets, *J. Geophys. Res.*, *106*, 21,549–21,554.

Zinn, J., C. D. Sutherland, and S. Ganguly (1990), The solar flare of August 18, 1979: Incoherent scatter radar data and photochemical model comparisons, *J. Geophys. Res.*, *95*, 16,705–16,718.

U. S. Inan and N. G. Lehtinen, Department of Electrical Engineering, Stanford University, Stanford, CA 94305, USA. (nleht@stanford.edu)